AIAA JOURNAL
Vol. 34, No. 2, February 1996

Experimental Studies of Supersonic Film Cooling with Shock Wave Interaction

Takeshi Kanda,* Fumiei Ono,† Masahiro Takahashi,‡ Toshihito Saito,† and Yoshio Wakamatsu§
National Aerospace Laboratory, Kakuda, Miyagi 981-15, Japan

The supersonic film cooling was tested in the Mach 2.35 wind tunnel to investigate the effect of the external shock wave on the film cooling. The coolant was injected with sonic speed. The weak shock wave with the pressure ratio of 1.21 did not reduce the film cooling effectiveness. The stronger shock wave with the pressure ratio of 1.44 decreased the effectiveness of the film cooling in the restricted region. The decrease of the effectiveness was mainly the result of the increase of the adiabatic wall temperature by the decrease of the local Mach number. The increase of the heat transfer coefficient must be considered as well as that of the adiabatic wall temperature. In the region of the interaction, energy and mass were not transferred, but the momentum was transferred from the primary flow to the coolant.

Nomenclature

C_H = Stanton number
Cp = specific heat
c_f = skin-friction coefficient
h_{inj} = height of film coolant injector at the exit
M = Mach number
P = pressure
PO = total pressure
q = heat flux
R = gas constant
r = recovery factor
T = temperature
TO = total temperature
u = velocity
x = axial distance from the coolant injector exit
y = perpendicular distance from the lower wall
$y1$ = y coordinate at 1 mm above the wall surface
γ = ratio of specific heats
η_{FC} = film cooling effectiveness defined in Eq. (1)
ρ = density
ϕ = mass fraction

Subscripts

aw = adiabatic wall
c = coolant
e = conditions at the edge of boundary layer
imp = shock wave impingement
local = local
pitot = pitot pressure
SG = shock generator
w = wall
∞ = primary flow
1 = upstream of the shock wave
2 = downstream of the shock wave and upstream of the reflected shock wave
3 = downstream of the reflected shock wave

Received May 16, 1995; presented as Paper 95-3141 at the AIAA/ASME/SAE/ASEE 31st Joint Propulsion Conference, San Diego, CA, July 10–12, 1995; revision received Oct. 16, 1995; accepted for publication Oct. 17, 1995.

*Senior Researcher, Ramjet Propulsion Research Division, Kakuda Research Center. Member AIAA.
†Researcher, Ramjet Structure Section, Ramjet Propulsion Research Division, Kakuda Research Center.
‡Researcher, Ramjet Structure Section, Ramjet Propulsion Research Division, Kakuda Research Center; currently Visiting Associate, Department of Mechanical Engineering, University of Queensland, Brisbane, Queensland 4072, Australia.
§Head, Ramjet Structure Section, Ramjet Propulsion Research Division, Kakuda Research Center. Member AIAA.

I. Introduction

THE film cooling is a well-known cooling method. It has widely been used, for example, in rocket engines, and it will be used in the scramjet engine.[1]

However, there are many unsolved problems with film cooling in the supersonic flow. One of the problems is the effect of the shock wave impingement on the coolant film.[2–5] It was reported that the shock wave impingement on the film cooling decreased the film cooling effectiveness.[3] In another report, the decrease of the effectiveness was very small when there was no separation.[5] In film cooling, there are inherent shock waves due to the thickness of the separating lip or the inequality of the static pressure between the coolant and the primary flow at the exit of the coolant injector. Therefore it should be made clear how the shock wave decreases the effectiveness of the film cooling.

In the present study, the film cooling was tested in the Mach 2.35 wind tunnel to study the effect of the external shock wave on the film cooling.

II. Experimental Apparatus and Methods

The Mach 2.35 blowdown-type wind tunnel, shown in Fig. 1, was used with the sonic injection of the coolant. The total temperature and the total pressure of the primary fluid, nitrogen, were approximately 280 K and 1400 kPa, respectively. The coolant, which was also nitrogen, was cooled in the heat exchanger by the liquid nitrogen. The total temperature and the total pressure of the coolant were approximately 230 K and 240 kPa, respectively. The design static pressure of the coolant at the injector exit was slightly higher than that of the primary flow of 100 kPa. The height of the coolant injector exit was 4 mm, and the thickness of the separating lip was 1.5 mm. The boundary-layer thickness of the primary flow was about

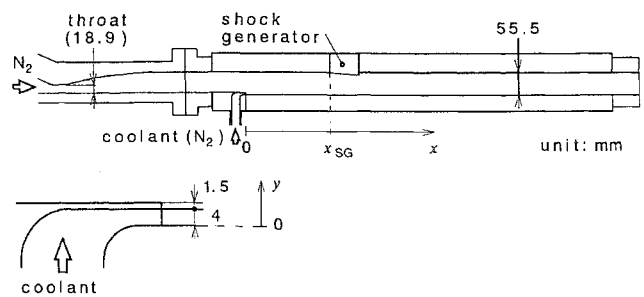

Fig. 1 Wind tunnel.

5 mm at the position of the coolant injector exit according to the pitot pressure measurement.

The recovery wall temperature was measured with thermocouples, whose diameter was 0.65 mm. The test section was made of Bakelite®, phenol-formaldehyde resin. Its thermal conductivity of 0.2 $W \cdot m^{-1} \cdot K^{-1}$ is much lower than that of the nickel alloy of 20 $W \cdot m^{-1} \cdot K^{-1}$. The adiabatic wall condition, therefore, seemed to be realized practically in the test section. The thermocouples were aligned at the center of the bottom wall with an interval of 10 mm. One of the thermocouples was located at $x/h_{inj} = 0.625$, which was nearest to the exit of the film coolant injector.

The width of the test section was 50 mm, whereas the height was 55.5 mm. The design mass flux ratio of the film coolant to the primary flow was 0.39. The unit Reynolds number of the primary flow and that of the coolant with sonic injection were 1.4×10^8 and 4.1×10^7 m^{-1}, respectively.

Two kinds of shock generators were used to investigate the effect of the shock wave strength. Table 1 shows the features of the shock generators. The pressure ratios shown in the table were calculated with the shock wave relation.

Table 1 Shock generator

Shock generator	Deflection angle, deg	P_2/P_1	P_3/P_1
1	3	1.21	1.44
2	6	1.44	2.02

Table 2 Shock generator 1 position

	Middle	Downstream
x_{SG}/h_{inj}	−2.5	85.0
x_{imp}/h_{inj}	21.3	107.5

Table 3 Shock generator 2 position

	Upstream	Middle	Downstream
x_{SG}/h_{inj}	−15.0	−5.0	82.5
x_{imp}/h_{inj}	3.5	14.3	102.0

The positions of the shock generators and the positions of the shock wave impingement are indicated in Tables 2 and 3. The positions of the shock generators were termed the upstream position, the middle position, and the downstream position as shown in the tables. The position of the shock wave impingement was the impinging point of the incident shock wave on the wall or against the separation shock wave according to the schlieren picture.

The wall pressure and the pitot pressure were measured with a rotary pressure scanner (Scanivalve®). The outer diameter of the pitot tube was 0.63 mm. The measured data were nondimensionalized with the total pressure in the reservoir of the wind tunnel. Both sides of the wind-tunnel test section held Pyrex® glass windows so that optical visualization such as a schlieren method could be carried out.

In the preliminary testing, the wall temperature was measured with an infrared-radiation thermometer, TVS-2000 (Nippon Avionics Co., Ltd.), around the coolant injector exit and around $x/h_{inj} = 100$. According to the temperature distribution, the two dimensionality of the wall temperature distribution was good.

III. Results

Figure 2 shows the spark schlieren photographs. In every experiment with shock generator (SG)1, the shock wave reflected simply on the wall of the wind tunnel. When SG2 was used at the upstream position or at the middle position, the shock wave reflected complicatedly, and it changed the structure of the interacting region from the quiet condition. There seems the separation shock wave from the coolant/mixing layer. When SG2 was used at the downstream position, the interacting region was small.

Figure 3 shows the pitot pressure distributions. The distributions were slightly affected by SG1 around the shock impinging position. The distribution was not affected by SG2 at the downstream position very much. That was strongly affected by SG2 at the upstream position and at the middle position.

The distributions of the total pressure and the wall pressure are shown in Fig. 4. When the total pressure was calculated with the wall pressure and the pitot pressure, it was assumed that the static pressure and the mass fraction at $y = y1$ were not very much different from the respective values on the wall.

Just behind the lip separating the primary flow from the coolant, there was wake, and both the coolant and the primary flow expanded toward the wake. According to the pitot pressure, wall pressure, and

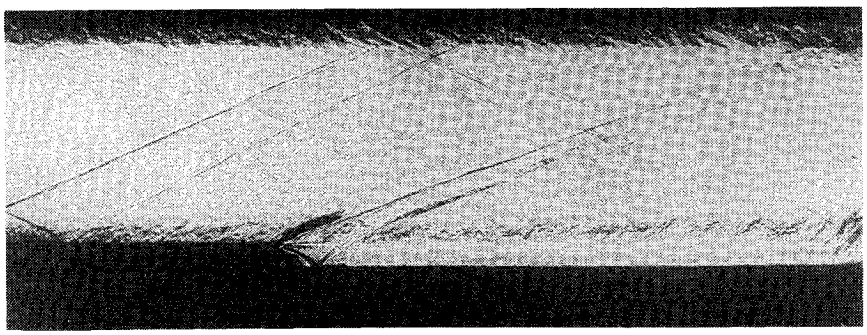

a) No shock generator

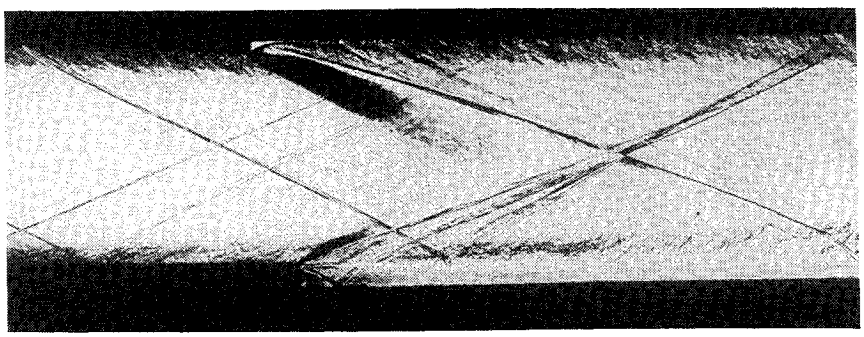

b) SG1 at upstream position

Fig. 2 Schlieren photographs.

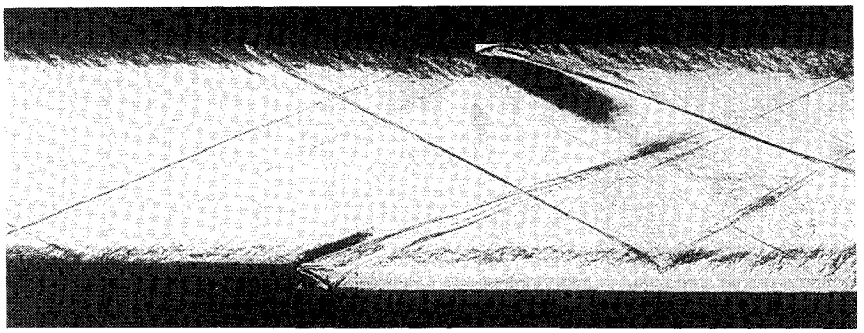

c) SG1 at middle position

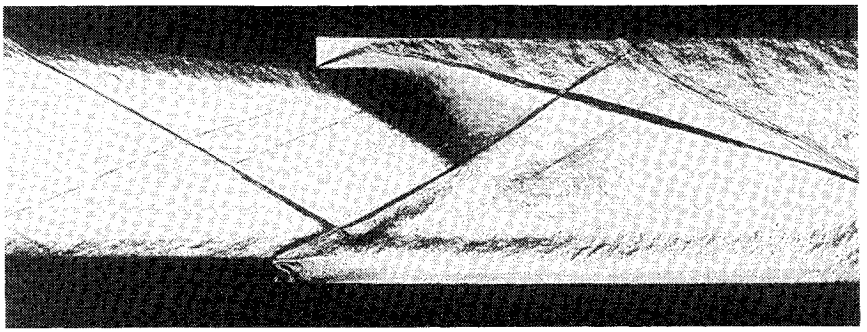

d) SG2 at upstream position

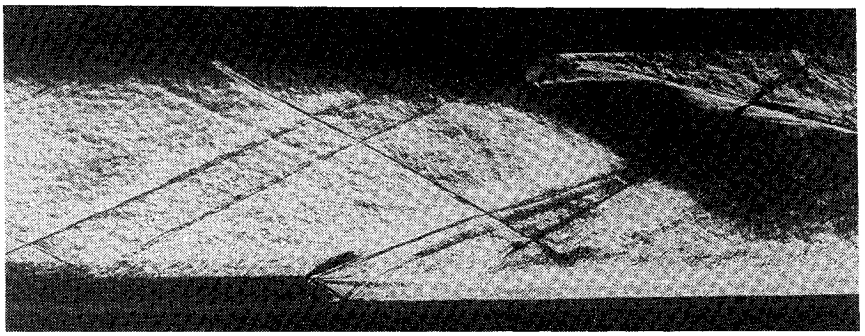

e) SG2 at middle position

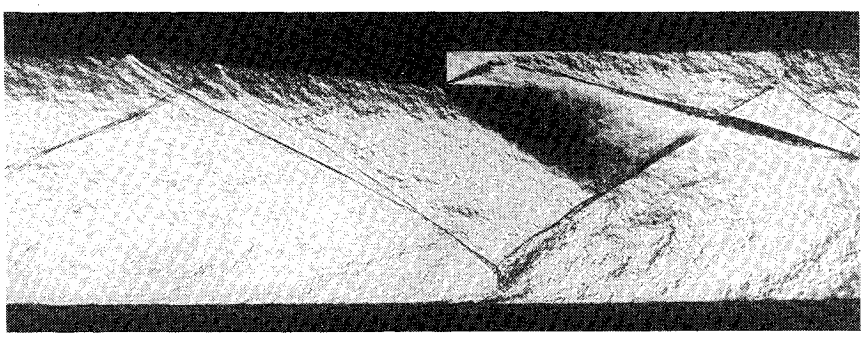

f) SG2 at downstream position

Fig. 2 (continued) Schlieren photographs.

schlieren photographs, the coolant, which was designed to be injected at the sonic speed, expanded to a supersonic speed. According to the wall pressure and the pitot pressure, the local Mach number of the coolant at $x/h_{\text{inj}} = 0.625$ was 1.2. Then the flows reflected and made shock waves. The coolant then decelerated across the shock wave and became subsonic behind the reflected shock wave. The steep wall pressure dip, which was observed in the vicinity of the coolant injector exit except when using SG2 at the upstream position, was because of the expansion wave and the shock wave. The mass flux ratio and the convective Mach number changed from 0.36 and 0.54 of the design values to 0.32 and 0.58, respectively.

When SG2 was at the upstream position and at the middle position, the increased wall pressures resulting from the shock wave impingement were greater than the total pressure of the coolant layer without the external shock wave impingement. The total pressure of the coolant layer increased around the region of the shock wave interaction.

Figure 5 shows the film cooling effectiveness. The film cooling effectiveness was defined as follows:

$$\eta_{FC} = \frac{T_{aw} - TO_{\infty}}{TO_c - TO_{\infty}} \tag{1}$$

The total temperature of the coolant was calculated from the adiabatic wall temperature and the Mach number at $x/h_{\text{inj}} = 0.625$. The adiabatic wall temperature is expressed as follows:

$$T_{aw} = TO_e \left\{ r + \frac{1 - r}{1 + (\gamma - 1)M_e^2/2} \right\} \tag{2}$$

Recovery factor was assumed to be 0.90.

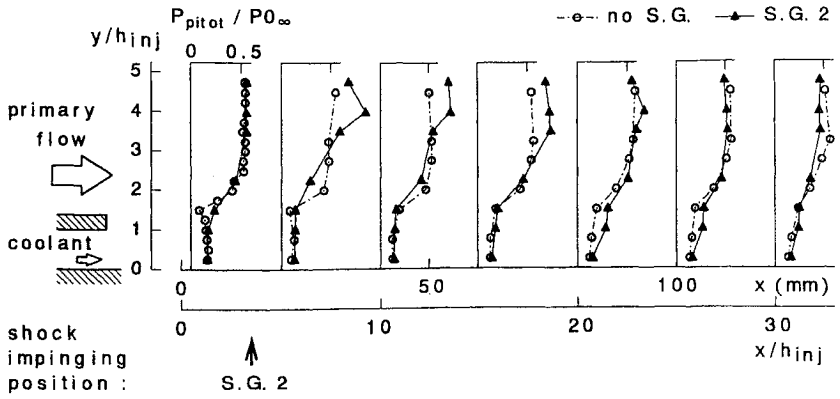

a) SG at upstream position

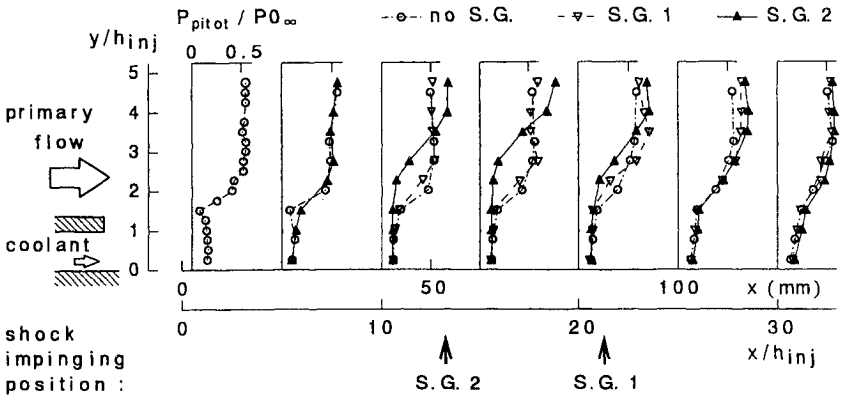

b) SG at middle position

Fig. 3 Pitot pressure distribution.

There are several kinds of definition of film cooling effectiveness.[6,7] The use of total temperature seems preferable to adiabatic wall temperature for the following reasons.

1) The adiabatic wall temperature of the coolant layer can vary very much because of expansion waves and shock waves in the vicinity of the coolant injector exit. Therefore, the choice of the position of the reference wall temperature is a very difficult problem. When total temperature is adopted, the reference temperature is specified simply.

2) When an experimental parameter, e.g., the injection Mach number of the coolant, is changed, the adiabatic wall temperature of the reference position changes. Consequently, when the adiabatic wall temperature is adopted as the reference temperature, the same local adiabatic wall temperature is evaluated as different film cooling effectiveness among the tests with different injection Mach numbers of the coolant. When the total temperature is adopted as the reference temperature, there is not such a problem.

When there was no external shock wave, the film cooling effectiveness was above unity at the upstream position. At the middle position, the effectiveness began to fall from unity, and it became about 0.5 at the downstream position. The drop of the film cooling effectiveness in the downstream region was -0.47 power of the distance x. The drop was -0.62 power when the local total temperature was used in Eq. (1) instead of the local adiabatic wall temperature T_{aw}. According to the analytical investigation based on change of the local total temperature,[6,8] the power of the drop of the film cooling effectiveness is -0.8 power of the distance. The power of several investigations scattered from -0.3 to -2.0, and most of the values were around -0.7.[1] The present value of -0.62 seems similar to other previous results.

The film cooling effectiveness scattered. There seem to be several reasons, e.g., the protrusion/hollow of the thermocouple from the wall surface. If there is the change of the wall temperature of 1 K, there is the change of the film cooling effectiveness of about 2% in this testing. When there was no shock generator, the film cooling effectiveness spread within about several percents. When there was a shock generator, there must be the fluctuating motion of the fluid in the separated region, and the spread of the film cooling effectiveness might be due to this unsteadiness.

There were no differences among the effectiveness when the shock generators (SGs) were located at the downstream position. SG1 did not affect the effectiveness. When SG2 was at the upstream position and at the middle position, the shock wave reduced the effectiveness about 10% in each testing. In the downstream of the shock wave impingement, however, the effectiveness recovered to that without the external shock wave.

IV. Discussion

A. Decrease of Film Cooling Effectiveness

When the coolant does not mix with the primary flow, the total temperature of Eq. (2) can be replaced by the total temperature of the coolant and Eq. (1) is expressed as follows:

$$\eta_{FC} = \left\{ r + \frac{1-r}{1+(\gamma-1)M_c^2/2} - \frac{TO_\infty}{TO_c} \right\} \Big/ \left\{ 1 - \frac{TO_\infty}{TO_c} \right\} \quad (3)$$

The assumption seems adequate in the vicinity of the coolant injector because the pitot pressure distributions near the wall were approximately uniform. Equation (3) indicates that when the Mach number is zero, the adiabatic wall temperature is equal to the total temperature, and the film cooling effectiveness is unity, and that the film cooling effectiveness increases more than unity as the Mach number increases. For example, when the Mach number is unity, the adiabatic wall temperature is $0.98 \times TO_c$, and the film cooling effectiveness becomes 1.08 with the testing conditions of the present study. When the Mach number is 2, then the effectiveness becomes 1.20. The film cooling effectiveness larger than unity was due to the smaller adiabatic wall temperature than the total temperature near the exit of the film coolant injector.

Figure 6 shows the Mach numbers at $y = y1$ calculated from wall pressure and the pitot pressure. The Mach number with the SG1 was around unity. The Mach number with the SG2 once became small and then increased because of the expansion wave from the trailing edge of the shock generator. The decrease of the Mach number

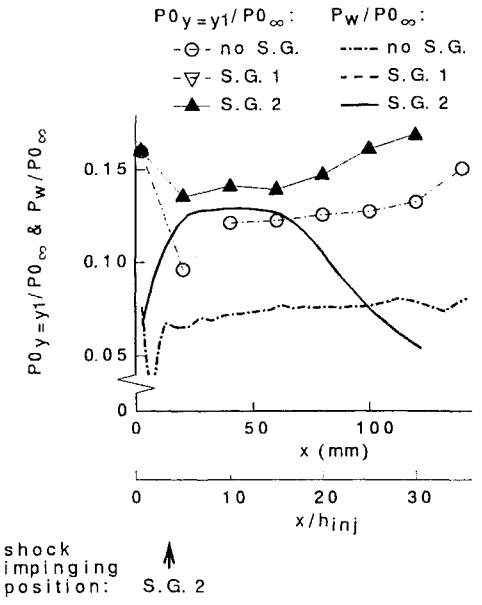

a) SG at upstream position

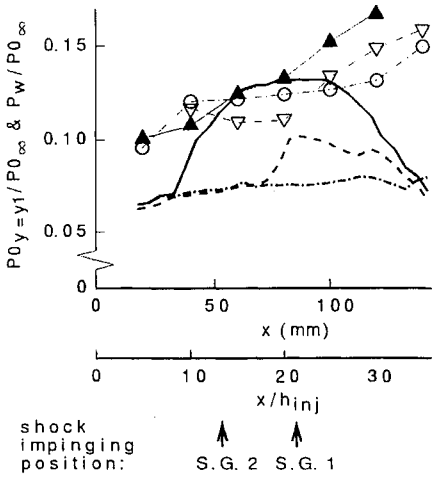

b) SG at middle position

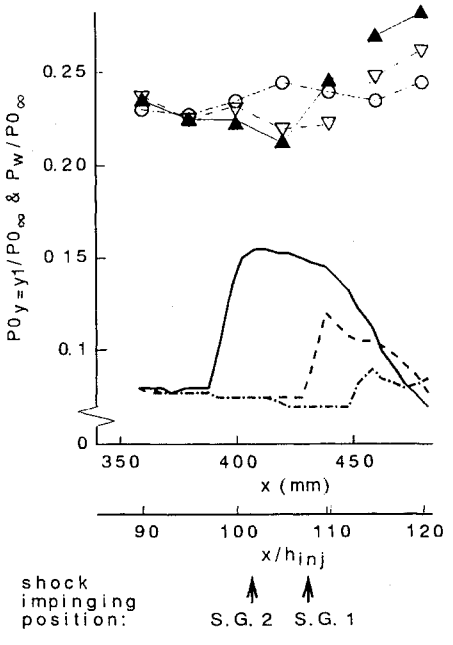

c) SG at downstream position

Fig. 4 Total pressure and wall pressure.

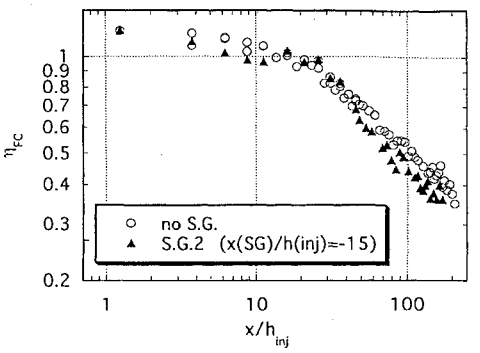

a) SG at upstream position

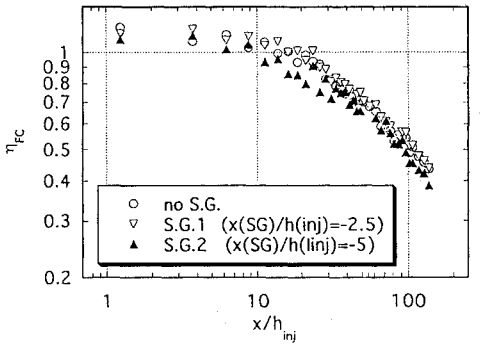

b) SG at middle position

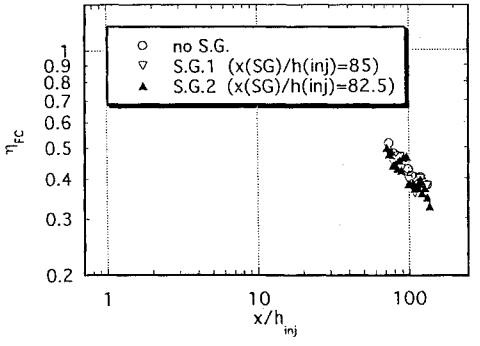

c) SG at downstream position

Fig. 5 Film cooling effectiveness.

shown in Fig. 6 can introduce the increase of the adiabatic wall temperature and the decrease of the film cooling effectiveness of about 10%. The decrease of the film cooling effectiveness shown in Fig. 5 was also about 10%. The decrease of the film cooling effectiveness in the downstream region seems to be the result of the entrainment of the primary flow,[8] but the decrease of the film cooling effectiveness in the interacting region seems mainly to be the result of the decrease of the local Mach number. Therefore, the film cooling effectiveness coincided with the effectiveness without the external shock wave downstream of the interaction.

This effect of local Mach number becomes small as the temperature ratio, TO_∞/TO_c, increases as can be seen in Eq. (3). Its value of the present testing was 1.2. When the ratio is 10, for example, the decrease of the film cooling effectiveness is only about 1% with a decrease of the Mach number from 3 to 0.

B. Heat Transfer Coefficient

In the actual device, the film cooling will be used with the regenerative cooling,[1] and there will be heat transfer from the film coolant to the wall. Therefore, the heat transfer coefficient is important as well as the adiabatic wall temperature on the heat transfer. But the film cooling effectiveness defined with Eq. (1) represents only the effect of the adiabatic wall temperature. When the adiabatic wall temperature is used to define the film cooling effectiveness, the effectiveness may be higher than when the heat flux is used. The different tendencies on the film cooling effectiveness with the shock wave interaction among several reports[3–5] may be the result of the change of the heat transfer coefficient.

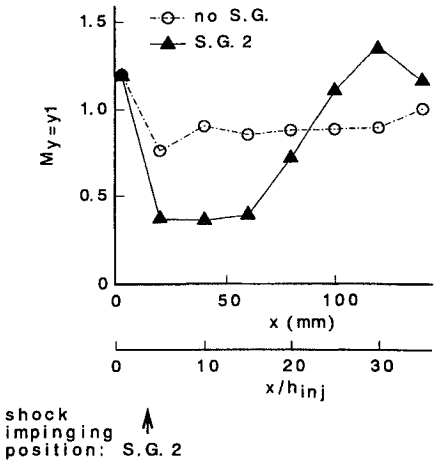

a) SG at upstream position

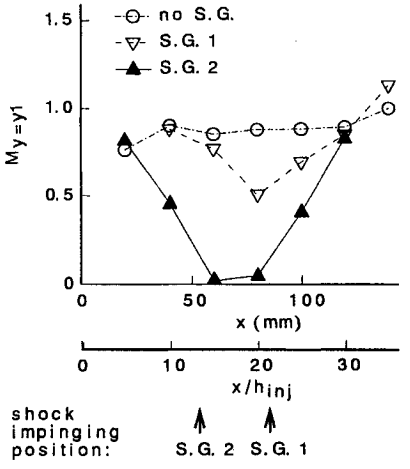

b) SG at middle position

Fig. 6 Mach number at $y = y1$.

The report by Holden et al.[3] seemed to show that the shock wave impingement destroys the effectiveness of film cooling. They measured heat flux instead of the adiabatic wall temperature. If their decrease of the film cooling effectiveness had no relation with increase of total temperature on the wall, the film cooling effectiveness can recover downstream of the shock wave impingement, and the effectiveness of film cooling can decrease extraordinarily in the interacting region with the shock wave, even though the total temperature of the coolant layer does not change very much. Consequently, we adopted the coolant Mach number of 4 and ratio of specific heats of 1.67 because of the experimental condition by Holden et al. in the following discussion.

We assumed that there was no mixing of the coolant with the primary flow, and the heat flux from the coolant to the wall is as follows:

$$q = \rho_e \cdot u_e \cdot C_H \cdot Cp(T_{aw} - T_w) \tag{4}$$

To investigate the increase of the heat flux across the shock wave impingement, the heat flux far downstream of the shock wave impingement, not at the interacting region, was compared with that upstream of the shock wave impingement. The Reynolds analogy was used to calculate the Stanton number. Assuming the Prandtl number is unity, Eq. (4) is rewritten as follows, using Eq. (2):

$$q = \frac{1}{2} c_f \cdot P_e \cdot M_e \sqrt{\frac{\gamma\{1 + (\gamma - 1)M_e^2/2\}}{R \cdot TO_e}} \times Cp \cdot TO_e \left\{ r + \frac{1 - r}{1 + (\gamma - 1)M_e^2/2} - \frac{T_w}{TO_e} \right\} \tag{5}$$

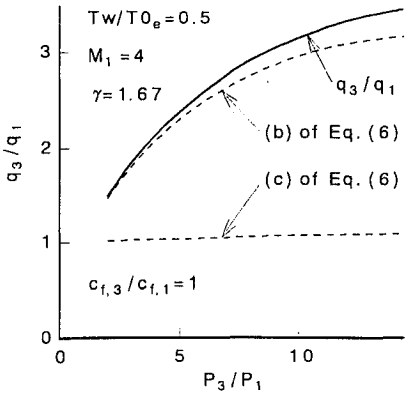

Fig. 7 Effect of shock wave on heat flux ratio.

The ratio of heat flux with the pressure increase resulting from the shock wave impingement to the flux without the pressure increase is as follows, assuming the total temperature is constant across the shock wave:

$$\frac{q_3}{q_1} = \underbrace{\frac{c_{f,3}}{c_{f,1}}}_{(a)} \underbrace{\frac{P_{e,3}}{P_{e,1}} \frac{M_{e,3}}{M_{e,1}} \sqrt{\frac{1 + (\gamma - 1)M_{e,3}^2/2}{1 + (\gamma - 1)M_{e,1}^2/2}}}_{(b)} \times \underbrace{\frac{r + \{(1 - r)/[1 + (\gamma - 1)M_{e,3}^2/2]\} - (T_w/TO_e)}{r + \{(1 - r)/[1 + (\gamma - 1)M_{e,1}^2/2]\} - (T_w/TO_e)}}_{(c)} \tag{6}$$

The (a) and (b) terms express the ratio of heat transfer coefficients, and the (c) term means the ratio of the temperature differences of $(T_{aw} - T_w)$. Figure 7 shows the ratio of the heat fluxes by Eq. (6). The downstream properties of the shock wave were calculated with the shock wave relation.

When there is no mixing of the coolant with the primary flow, the increase of the heat flux was mainly because of the increase of the heat transfer coefficient. The decrease of the Mach number resulting from the external shock wave does not affect the adiabatic wall temperature very much. The unit Reynolds number does not change very much across the shock wave, whereas the skin-friction coefficient increases because of the decrease of the Mach number,[9] and so the heat flux will become larger downstream of the shock wave. Actually, according to the experimental results on the turbulent boundary-layer/shock wave interaction, the peak heat flux is roughly proportional to 0.85 power of the peak pressure, and the heat flux is nearly equal to the peak flux downstream of the shock wave impingement.[10] The heat transfer coefficient must be considered as well as the adiabatic wall temperature in the shock wave interaction. The increase of the heat flux reported by Holden et al.[3] is still larger than the calculated value shown in Fig. 7, and so there are additional causes for the increase of the heat flux resulting from the shock wave impingement.

C. Mixing Enhancement

There are several reports that the turbulence increases downstream of the shock wave in the turbulent boundary layer[11–13] and in the turbulent shear layer.[14] If the turbulence increased behind the shock wave, the mixing may be enhanced, the local total temperature may increase, and the film cooling effectiveness may decrease. The distance from the wall surface to the point $y1$, where the nearest pitot probe to the wall was located, was small, comparing the height of the mixing layer. Consequently, assuming that the mixing rate at the point was, not very much different from that on the wall, the local total temperature at $y = y1$ was calculated from the wall temperature and the Mach number with Eq. (2) to investigate the mixing rate. Then, with the local total temperature, the coolant mass fraction was calculated with the following equation, assuming the heat was transferred mainly due to mixing:

$$TO_{\text{local}} = \phi_c TO_c + (1 - \phi_c)TO_\infty \tag{7}$$

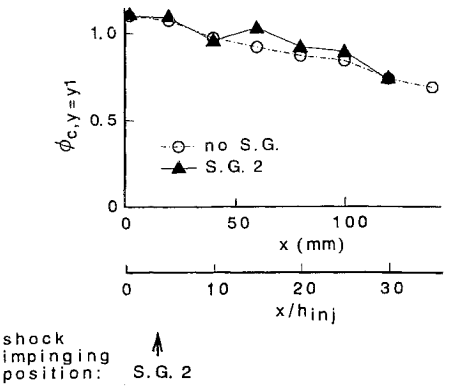

a) SG at upstream position

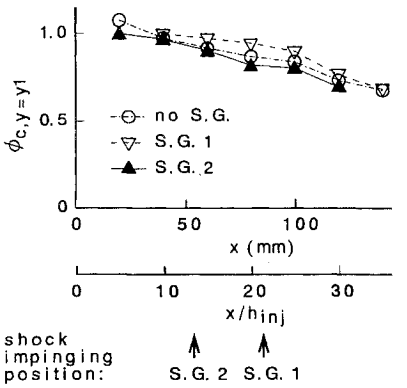

b) SG at middle position

Fig. 8 Mass fraction.

Figure 8 shows the calculated mass fraction of the coolant at $y = y1$. The mass fractions of the coolant of the flows with or without the external shock waves were approximately the same. If the decrease of the film cooling effectiveness is induced by an increase of mixing, and there is no change in the local Mach number, the 5% decrease of the film cooling effectiveness can be obtained by about 10% decrease of the mass fraction of the coolant in this testing. If the mixing was dominant, the recovery of the film cooling effectiveness shown in Fig. 5 could not be observed. The mixing seems not to be enhanced near the wall in the interacting region.

There seemed to be the following causes in error of mass fraction, e.g., the value more than unity near the coolant injector exit.

1) There was about 2 K difference in temperature indication among thermocouples. It might bring about 4% difference of the mass fraction by Eq. (7).

2) The Mach number changed very much in the vicinity of the coolant injector exit as shown in Figs. 6a and 6b, even though there was no external shock wave. Consequently, there could be the error of Mach number of about 0.2 there. There was about 4% difference of the mass fraction when there was about 0.2 difference in Mach number.

Therefore, there could be about 8% error of the mass fraction. Many assumptions went into the present analysis of the mass fraction, and the result seems to lack satisfactory accuracy. The change of mass fraction must be investigated in another way, e.g., by gas sampling.

D. Increase of Total Pressure

According to the total pressure distribution of Fig. 4, when there was large pressure increase due to the shock wave, the momentum was transported from the primary flow to the coolant layer quickly in the interacting region, but neither the mass nor the energy were in the present study. We have not made clear the difference of mechanisms between the momentum transportation and the energy/mass transportation.

V. Conclusions

The effect of the external shock wave on the film cooling was investigated in the Mach 2.35 wind tunnel, and the following conclusions were made clear.

1) There was little effect by the external weak shock wave of the pressure ratio of 1.21. The shock wave of the pressure ratio of 1.44 decreased the film cooling effectiveness.

2) The decrease of the film cooling effectiveness was mainly the result of the decrease of the local Mach number.

3) The increase of the heat transfer coefficient should be considered, as well as that of the adiabatic wall temperature in the interacting region.

4) Neither the mass nor the energy was transferred, whereas the momentum was transferred from the primary flow to the coolant layer in the interacting region.

Acknowledgments

The authors would like to thank Goro Masuya of the National Aerospace Laboratory (currently Tohoku University) and Nobuo Chinzei of National Aerospace Laboratory for discussions.

References

[1]Kanda, T., Masuya, G., Ono, F., and Wakamatsu, Y., "Effect of Film Cooling/Regenerative Cooling on Scramjet Engine Performances," *Journal of Propulsion and Power*, Vol. 10, No. 5, 1994, pp. 618–624.

[2]Alzner, E., and Zakkay, V., "Turbulent Boundary-Layer Shock Interaction with and Without Injection," *AIAA Journal*, Vol. 9, No. 9, 1971, pp. 1769–1776.

[3]Holden, M. S., Nowak, R. J., Olsen, G. C., and Rodriguez, K. M., "Experimental Studies of Shock Wave/Wall Jet Interaction in Hypersonic Flow," AIAA Paper 90-0607, Jan. 1990.

[4]Olsen, G. C., Nowak, R. J., Holden, M. S., and Baker, N. R., "Experimental Results for Film Cooling in 2-D Supersonic Flow Including Coolant Delivery Pressure, Geometry, and Incident Shock Effects," AIAA Paper 90-0605, Jan. 1990.

[5]Juhany, K., and Hunt, M. L., "Flowfield Measurements in Supersonic Film Cooling Including the Effect of Shock-Wave Interaction," *AIAA Journal*, Vol. 32, No. 3, 1994, pp. 578–585.

[6]Goldstein, R. J., "Film Cooling," *Advances in Heat Transfer*, Vol. 7, Academic, New York, 1971, pp. 326–329.

[7]Juhany, K. A., Hunt, M. L., and Sivo, J. M., "Influence of Injectant Mach Number and Temperature on Supersonic Film Cooling," *Journal of Thermophysics and Heat Transfer*, Vol. 8, No. 1, 1994, pp. 59–67.

[8]Hartnett, J. P., Birkebak, R. C., and Eckert, E. R. G., "Velocity Distributions, Temperature Distributions, Effectiveness and Heat Transfer for Air Injected Through a Tangential Slot into a Turbulent Boundary Layer," *Journal of Heat Transfer*, Vol. 83, No. 3, 1961, pp. 293–306.

[9]White, F. M., "Viscous Fluid Flow," McGraw–Hill, New York, 1974, pp. 637, 638.

[10]Holden, M. S., "Shock Wave-Turbulent Boundary Layer Interaction in Hypersonic Flow," AIAA Paper 72-74, Jan. 1972.

[11]Anyiwo, J. C., and Bushnell, D. M., "Turbulence Amplification in Shock-Wave Boundary-Layer Interaction," *AIAA Journal*, Vol. 20, No. 7, 1982, pp. 893–899.

[12]Hayakawa, K., Smits, A. J., and Bogdonoff, S. M., "Hot-Wire Investigation of an Unseparated Shock-Wave/Turbulent Boundary-Layer Interaction," *AIAA Journal*, Vol. 22, No. 5, 1984, pp. 579–585.

[13]Zang, T. A., and Bushnell, D. M., "Numerical Computations of Turbulence Amplification in Shock-Wave Interactions," *AIAA Journal*, Vol. 22, No. 1, 1984, pp. 13–21.

[14]Lu, P. J., and Wu, K. C., "On the Shock Enhancement of Confined Supersonic Mixing Flows," *Physics of Fluids A*, Vol. 3, No. 12, 1991, pp. 3046–3062.